

Mechanism of the Electrodeposition of Cobalt(II) Thiocyanate in N,N-Dimethylformamide (DMF) Solution and Effect of Chloride Ions

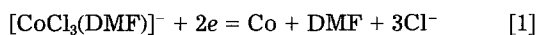
C. Q. Cui, S. P. Jiang, and A. C. C. Tseung*

Chemical Energy Research Centre, Department of Chemistry and Biological Chemistry, University of Essex, Wivenhoe Park, Colchester CO4 3SQ, England

ABSTRACT

The deposition process of cobalt from cobalt(II) thiocyanate solution in N,N-dimethylformamide (DMF) with the addition of Cl⁻ ions has been investigated. In Co(NCS)₂ DMF solution, cobalt(II) ions exist in the form of [CoNCS(DMF)₅]⁺ and [Co(NCS)₄]²⁻ and the former is the main electroactive species for the deposition of cobalt. The mechanism of the deposition of cobalt from Co(NCS)₂ DMF solutions is via under electron-transfer/mass-transfer control. As Cl⁻ ions are added, Cl⁻ ions act as a competitive ligand substitute for NCS⁻ ions within [CoNCS(DMF)₅]⁺, which leads to the decrease of the [CoNCS(DMF)₅]⁺ concentration, thus inhibiting the deposition process of cobalt. The deposition of cobalt in nonaqueous solutions greatly depends on the nature of metal ion complexes with anions in the solution. Anions which act as competitive ligands participate in the complexation equilibria in nonaqueous solution and directly influence the form and the concentration of the electroactive complex species. In conclusion, the effect of anions added in the deposition of metal in nonaqueous solution greatly depends on the nature of metal ion complexes and is much greater than the one in aqueous solutions.

In our previous work on the electrodeposition of cobalt(II) chloride in N,N-dimethylformamide (DMF) solution (1), it was found that chloride ions have a significant effect on the rate of deposition of cobalt from cobalt(II) chloride in DMF solution. In the presence of chloride ions, DMF molecules within the octahedral [Co(DMF)₆]²⁺ solvents are successively replaced by Cl⁻ ions to form various coordination complexes. The ionization equilibria of cobalt(II) chloride in DMF and the stability of the cobalt(II) chloride complexes have been extensively studied (2-8). However, the electrolytic properties of the solution are controlled by the complex [Co(DMF)₆]²⁺ · 2[CoCl₃(DMF)]⁻ (4). Deposition of cobalt from CoCl₂ in DMF proceeds mainly through the electroreduction of [CoCl₃(DMF)]⁻ (1)



It has been shown (1) that the accumulation of the chloride ions formed at the electrode surface could considerably increase the concentration of [CoCl(DMF)₅]⁺ through the substitution reaction



Thus, the deposition process also occurs via a single two-electron step for electroreduction of [CoCl(DMF)₅]⁺



This has been confirmed by the occurrence of the cathodic peak on the reverse scans during cyclic voltammetric experiments in CoCl₂ solutions in DMF (1). Therefore, in DMF the electroactive components are mainly [CoCl₃(DMF)]⁻ and [CoCl(DMF)₅]⁺, even though the initial concentration of [CoCl(DMF)₅]⁺ is very low. This is due to the very low formation constant for [CoCl(DMF)₅]⁺ (log β = 3.5), as compared to that for [CoCl₃(DMF)]⁻ (log β = 11) (4). The exchange between the cobalt(II) chloride complexes could simultaneously take place at the electrode surface due to the constant change of the chloride ions during the deposition process (see reactions [1]-[3]). Also, when the concentration ratio of Cl⁻ to cobalt(II) is much higher than 2, cobalt(II) chloride is present as [CoCl(DMF)₅]⁺, [CoCl₂(DMF)₂], [CoCl₃(DMF)]⁻, and [CoCl₄]²⁻ in DMF (5).

Since the thiocyanate ion is a strong ligand, the influence of the donor number of the solvent on the stabilities of the complex ions will therefore be small. Indeed, as shown in (6), cobalt(II) ions in DMF solution of cobalt(II) thiocyanate exist in the form of [CoNCS(DMF)₅]⁺ and [Co(NCS)₄]²⁻ complexes. The formation constants are log

β₁ = 4.5 and log β₄ = 12.2, respectively. The high stability of the tetrahedral [Co(NCS)₄]²⁻ complex leads to the formation of 2[CoNCS(DMF)₅]⁺ · [Co(NCS)₄]²⁻ complex electrolytes in solutions of Co(NCS)₂ in DMF.

Since it seems that the formation of the electroactive chloro complexes of cobalt(II) in DMF is also dependent on the concentration ratio of Cl⁻ to cobalt(II), it would be interesting to study the effect of chloride ions in DMF solvent on the electrodeposition of cobalt(II) and to study the electrochemical behavior of various kinds of cobalt(II) complexes in DMF solutions. In addition, such studies will highlight the differences between the deposition of metals in nonaqueous and aqueous solution. In the present paper, the effect of chloride ions on the electrodeposition of cobalt(II) in DMF solution will be studied by changing the concentration ratio of chloride ions to cobalt(II) ions in the solution by adding anhydrous LiCl to a base solution of 0.1M Co(SCN)₂ + 0.5M LiClO₄ in DMF.

Experimental

Nickel rod with a surface area of 0.283 cm² with the cylindrical side enclosed with PTFE was used as a working electrode. Cobalt foil (99.5%, supplied by Cobalt Development Institute) was used as the counterelectrode. An aqueous saturated calomel electrode (SCE) was used as the reference electrode which was connected to the cell with an agar-agar bridge. The electrochemical cell setup and the pretreatments of the working, counter, and reference electrodes were the same as in a previous paper (1).

All the chemicals used, LiCl (Aldrich), Co(SCN)₂ (BDH), and LiClO₄ (BDH), were anhydrous analytical grade. DMF was obtained from a commercial source (99%, Aldrich) and was not treated further.

The measurements were carried out using a rotating nickel disk electrode at room temperature. Cyclic voltammetry was generally started from a potential of -0.42 V (vs. SCE) and the potential was swept in the cathodic direction initially. For potentiostatic current-time transient measurements, the pulse potential was also started from -0.42 V. Additional details of the electrochemical techniques used were described elsewhere (1).

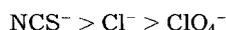
UV absorption spectra of the solutions were measured with a Phillips MPS-2000 spectrophotometer equipped with a PC-9801VM computer which recorded data at 2 nm intervals over the wavelength range 400-800 nm using a silicon dioxide glass cell with a pathlength of 1 cm. DMF solvent was used as the background. A Model 4070 conductivity meter (Jenway, Limited, England) was used to measure the electrical conductivity of the solution.

*Electrochemical Society Active Member.

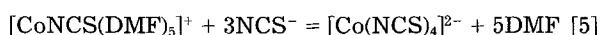
Results and Discussion

Physical chemistry properties of the solutions.—Figure 1 shows the visible absorption spectra of a series of DMF solutions of $3 \cdot 10^{-3}M$ $Co(NCS)_2$ + $1.5 \cdot 10^{-2}M$ $LiClO_4$ with various amounts of $LiCl$ ($0.3 \cdot 10^{-2}M$). The spectra of the $3 \cdot 10^{-3}M$ $Co(NCS)_2$ + $1.5 \cdot 10^{-2}M$ $LiClO_4$ solution in DMF without any $LiCl$ consists of two bands with maxima at 588 nm (shoulder peak, peak I) and 624.8 nm (peak II). The characteristics of this spectra are the same as the one observed in $Co(NCS)_2$ solutions in DMF (6). The band position, contour, and high intensity are typical of cobalt(II) in a tetrahedral environment (4, 9). The octahedral complex $[CoNCS(DMF)_5]^+$ could also be formed with relatively low absorptivity and negligible effect on the measured spectrum due to the thiocyanate complex of cobalt(II). This is indicated by the relatively low formation constant for complex $[CoNCS(DMF)_5]^+$ ($\log \beta = 4.5$) in the $Co(NCS)_2$ DMF solutions (6). Furthermore, this also shows that $LiClO_4$ only functions as the supporting electrolyte in this case.

With the addition of $LiCl$ to $3 \cdot 10^{-3}M$ $Co(NCS)_2$ + $1.5 \cdot 10^{-2}M$ $LiClO_4$ solution in DMF, the band intensity increases and more significantly, the band position shifts positively. This indicates the formation of different absorbing species due to the addition of chloride ions. When the concentration of $LiCl$ is higher than $0.015M$, significant changes in the spectra of the solution occur, developing a new maximum at 670.9 nm accompanied by the disappearance of the peak at 588 nm. The band positions of the spectra are quite close to the one observed in the case of $CoCl_2$ solutions in DMF (4), indicating the formation of the tetrahedral chloro-complex, $[CoCl_3(DMF)]^-$, in the $Co(NCS)_2$ - $LiClO_4$ - $LiCl$ -DMF system. The formation of cobalt(II) chloride complexes of $[CoCl_3(DMF)]^-$ and $[CoCl(DMF)_5]^+$ has been reported in the $Co(ClO_4)_2$ - Et_4NCl -DMF system when the Cl^-/Co^{2+} ratio was less than 2 (5). The coordination strength of anions as competitive ligands in descending order is as follows (2)



The above results suggest that $[Co(NCS)_4]^{2-}$ is the most stable complex species in the solution. However, the cobalt(II) chloride complex, $[CoCl_3(DMF)]^-$, can also be formed as the result of Cl^- ions, though the concentration could be very low and is largely dependent on the Cl^-/NCS^- ratio. The equilibria between complexes may be established as follows



The above conclusion is also supported by the change in conductivity of the solutions with the varying concentration of Cl^- ion added to $0.1M$ $Co(NCS)_2$ + $0.5M$ $LiClO_4$ solution in DMF (Fig. 2). The conductivity was determined by adding $LiCl$ to a fixed volume of $0.1M$ $Co(NCS)_2$ + $0.5M$ $LiClO_4$ DMF solution. As shown in Fig. 2, the conductivity of the solutions increases as the Cl^- ion concentration is increased, but decreases after the concentration of Cl^- ion reaches $0.5M$. The increase in conductivity is due to the increase of the concentration of the ionic species in the solution such as Cl^- ions. When the concentration of Cl^- reaches $0.5M$, reactions [4] and [5] could become significant. This leads to the decrease in the concentration of noncoordinated ionic species. Also, the concentration of complex species such as $2[CoNCS(DMF)_5]^+ \cdot [Co(NCS)_4]^{2-}$ and $2[CoCl_3(DMF)]^- \cdot [Co(DMF)_6]^{2+}$ could be significantly increased. The ionic strength of the solution is decreased and therefore results in the decrease of the ion concentration in the solution. Therefore, the conductivity of the solution is reduced.

According to the above discussions, it may be concluded that: (i) $[CoCl_3(DMF)]^-$ complex species is formed when Cl^- ions are added to $Co(NCS)_2$ solution in DMF; and (ii) as the concentration of Cl^- ions increases in cobalt(II) thiocyanate DMF solution, the concentration of

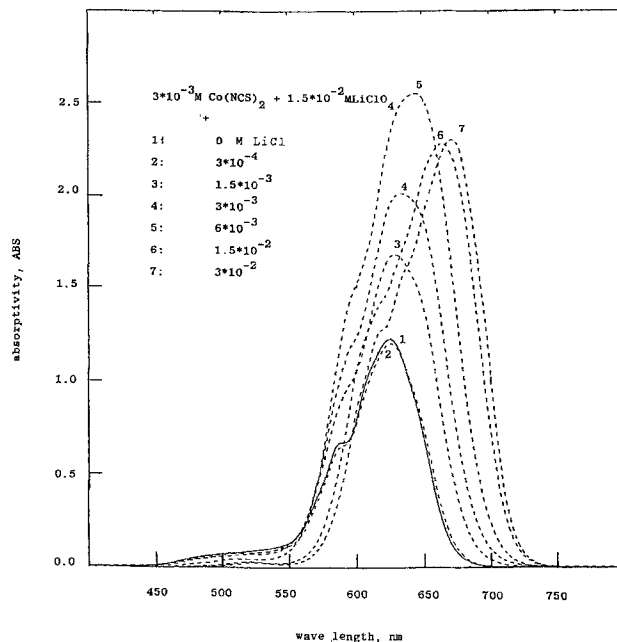


Fig. 1. Absorption spectra of $3 \cdot 10^{-3}M$ $Co(NCS)_2$ + $1.5 \cdot 10^{-2}M$ $LiClO_4$ added $LiCl$ solutions in DMF at $20^\circ C$. The concentrations of $LiCl$ are listed in the figure.

$[CoNCS(DMF)_5]^+$ decreases, but the concentrations of $[CoCl_3(DMF)]^-$ and $[Co(NCS)_4]^{2-}$ increase.

Mechanism for the deposition of cobalt from $Co(NCS)_2$ DMF solutions.—Figure 3 shows the cyclic voltammograms for the deposition of cobalt on a nickel disk electrode obtained using different cathodic reverse potentials at a scan rate of 10 mV/s in a $0.1M$ $Co(NCS)_2$ + $0.5M$ $LiClO_4$ DMF solution. The electrode was not rotated. There is virtually no cathodic current on the forward scans until the onset of the nucleation of cobalt ions (-1.84 V) and a rapid rise of current on the forward scans once the nucleation begins. Crossover between the cathodic and anodic current on the reverse scans also occurs as was observed in the deposition of cobalt from DMF and aqueous solutions of $CoCl_2$ (1, 10). These features show typical characteristics of a mechanism of nucleation and three-dimensional crystal growth (11, 12). It is also seen from Fig. 3 that the crossover potential shifts slightly to the cathodic side as the reverse potential changes cathodically. Such a change in the crossover potential with the potential of reversal was also observed in the deposition of mercury in aqueous solutions (12). This is due to the decrease of the surface concentration of the reactant and the deposition reactions are mainly controlled by the mass-transfer process (12). However, there are some basic differences for the deposition of cobalt in DMF solutions of $Co(NCS)_2$ and $CoCl_2$. In

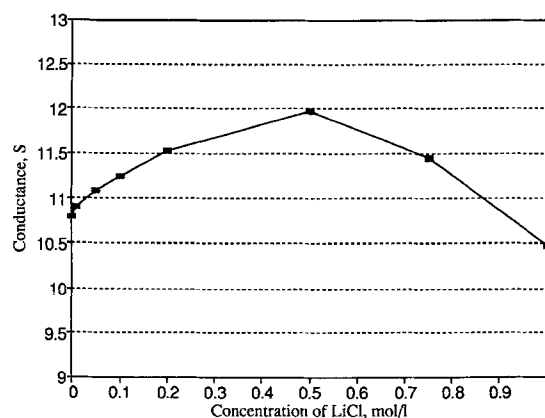


Fig. 2. Plot of the conductance as a function of the concentration of $LiCl$ added to $0.1M$ $Co(NCS)_2$ + $0.5M$ $LiClO_4$ solution in DMF at $20^\circ C$.

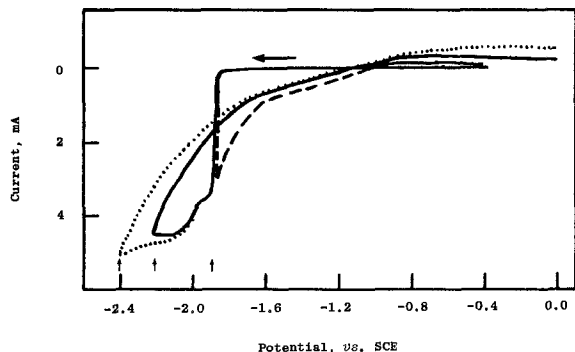


Fig. 3. Cyclic voltammograms obtained by changing the cathodic reverse potential at a scan rate of 10 mV/s in a 0.1M Co(NCS)₂ + 0.5M LiClO₄ DMF solution. The position of the reverse potential is indicated by the arrows.

the case of the latter, a shoulder peak occurs on the reverse scans. This shoulder peak has been attributed to the electroreduction of [CoCl(DMF)₅]⁺ in CoCl₂ solutions in DMF (1). The crossover potential shifts anodically as the reverse potential changes in the cathodic side in the case of CoCl₂ DMF solution. This is largely due to the catalytic effect of the Cl⁻ ions accumulated at the electrode surface on the reduction of electroactive species [CoCl₃(DMF)]⁻ and [CoCl(DMF)₅]⁺ (1).

The onset potential for the nucleation of cobalt ions from Co(NCS)₂ DMF solutions is depressed to about -1.84 V, which is much lower than the one for electrodeposition of cobalt in CoCl₂ DMF system (-1.16 V) (1). One of the reasons could be due to the relatively low concentration of the electroactive species. As shown in Fig. 3, there are two limiting reduction current plateaus for the deposition of cobalt from Co(NCS)₂ DMF solution, indicating the existence of two different electroactive species. It seems most likely that the electrodeposition of cobalt is at first through the reduction of [CoNCS(DMF)₅]⁺, which has much lower formation constant (log β₁ = 4.5) compared to that of [Co(NCS)₄]²⁻ (log β₄ = 12.2) (6). It is known that the change of the potential from the equilibrium is dependent on the formation constant β of the complex. The standard equilibrium potential for [Co(NCS)₄]²⁻ is therefore lower than that of [CoNCS(DMF)₅]⁺. This could imply that the second limiting current plateau is largely due to the reduction of [Co(NCS)₄]²⁻ at lower cathodic potential. The occurrence of the limiting reduction currents also confirms the importance of the mass-transfer process in the deposition of cobalt from Co(NCS)₂ DMF solution. On the other hand, for cyclic voltammograms measured in a 0.1M Co(NCS)₂ + 0.5M LiClO₄ DMF solution in the potential range of -2.20 to 0 V at a scan rate of 20 mV/s, the cathodic current measured at -2.2 V increases with an increase in the rotation rate of the electrode (Fig. 4). When the rotation rate increases above 5 Hz, the cathodic current becomes inde-

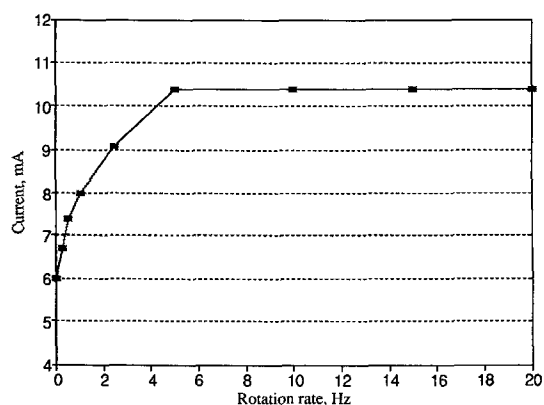


Fig. 4. Effect of rotation rate of the electrode on the cathodic current measured at -2.2 V on cyclic voltammograms obtained from a 0.1M Co(NCS)₂ + 0.5M LiClO₄ DMF solution at a scan rate of 20 mV/s.

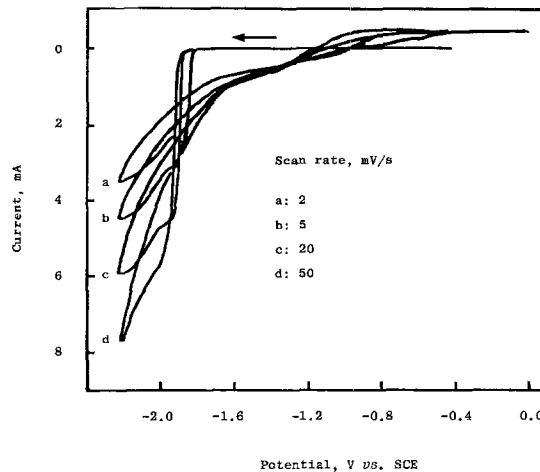


Fig. 5. Cyclic voltammograms for the deposition of cobalt from 0.1M Co(NCS)₂ + 0.5M LiClO₄ DMF solution measured at different scan rates.

pendent of the rotation rate. This also indicates that the deposition of cobalt from Co(NCS)₂ DMF solution is under electron transfer and mass-transfer control.

Figure 5 contains the cyclic voltammograms for the deposition of cobalt from a 0.1M Co(NCS)₂ + 0.5M LiClO₄ DMF solution using different scan rates. During the forward scan the cathodic current sharply increases once nucleation begins, reflecting the increase in nuclei density. As the potential sweeps further to the cathodic side, the corresponding cathodic current increases slowly and this could be related to the crystal growth in the deposition process. Nevertheless, the cathodic current increases as the scan rate increases. In the case of either a reversible or irreversible electrode reaction, the current at any potential in the linear voltammetric sweep is proportional to the concentration of reactant, C, and the square root of scan rate, v^{1/2}, if the mechanism for the electrode process only involves electron-transfer or mass-transfer processes (13). Figure 6 shows the plots of the cathodic currents measured at -2.2 V vs. scan rates in 0.1M Co(NCS)₂ + 0.5M LiClO₄ DMF solutions with and without the addition of 0.01M LiCl. The cyclic voltammetric curves were determined in a potential range of -0.42 and -2.2 V and the electrode was not rotated. It can be seen that a linear relationship exists between the cathodic current and v^{1/2}. In contrast, no such linear relationship between the cathodic current and v^{1/2} was observed in the case of CoCl₂ DMF solutions (1). This has been explained by the involvement of a catalytic process of Cl⁻ ions accumulated at the electrode surface, which significantly increases the concentration of electroactive species (reactions [2]-[3]). Consequently, the existence of the linear relationship between the cathodic

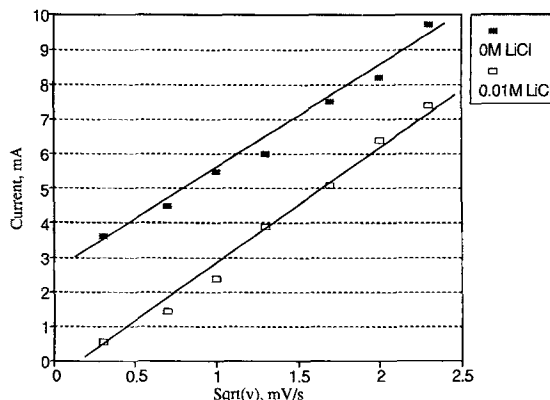


Fig. 6. Plots of the cathodic current measured at -2.2 V against the square root of scan rate. The cyclic voltammetric curves were obtained in 0.1M Co(NCS)₂ + 0.5M LiClO₄ DMF solutions with and without the addition of 0.01M LiCl.

current and $v^{1/2}$ in turn confirms that the deposition of cobalt from $\text{Co}(\text{NCS})_2$ DMF solution does not involve the catalysis mechanism as in the case of deposition of CoCl_2 DMF solutions (1), irrespective of the addition of chloride ions.

The mechanism for the deposition of cobalt from $\text{Co}(\text{NCS})_2$ DMF solutions is not the same as ones for the deposition of cobalt from CoCl_2 DMF solution, i.e., the effect of NCS^- ions on the deposition of cobalt is not the same as the Cl^- ions. The reason may be the existence of cobalt(II) complexes with competitive ligands contributing to the formation of the electroactive complexes in the deposition of cobalt. In $\text{Co}(\text{NCS})_2$ DMF solutions, the NCS^- ions produced at the electrode surface would mainly lead to the formation of more stable $[\text{Co}(\text{NCS})_4]^{2-}$ complex, which is less electrochemically active than $[\text{CoNCS}(\text{DMF})_5]^+$. Therefore, the thiocyanate ions accumulated at the electrode surface mainly due to the reduction of electroactive species, $[\text{CoNCS}(\text{DMF})_5]^+$, has little catalytic effect on the deposition process. The deposition of cobalt from $\text{Co}(\text{NCS})_2$ DMF solution involves a mechanism of nucleation and crystal growth under electron-transfer and mass-transfer control, which is the same as in the deposition of cobalt chloride in aqueous solution (10).

Effect of Cl^- ions as a competitive ligand.—Figure 7 compares the cyclic voltammograms for the deposition of cobalt at a scan rate of 10 mV/s in the DMF solutions of 0.1M $\text{Co}(\text{NCS})_2 + 0.5\text{M LiClO}_4$, 0.1M $\text{Co}(\text{NCS})_2 + 0.5\text{M LiClO}_4 + 1\text{M LiCl}$ and 0.1M $\text{CoCl}_2 + 0.5\text{M LiClO}_4$. In 0.1M $\text{CoCl}_2 + 0.5\text{M LiClO}_4$ solution, there is a cathodic peak at -1.42 V on the reverse scan which most probably corresponds to the reduction of $[\text{CoCl}(\text{DMF})_5]^+$ (reaction [3]) (1). On the other hand, there is no cathodic peak in the other two solutions on the reverse scans. This result is in agreement with the UV spectroscopy data (Fig. 1) that also indicates that the addition of Cl^- to $\text{Co}(\text{NCS})_2$ does not produce the $[\text{CoCl}(\text{DMF})_5]^+$ complex. However, upon addition of 1M LiCl to 0.1M $\text{Co}(\text{NCS})_2 + 0.5\text{M LiClO}_4$ DMF solution, the onset potential for the deposition of cobalt is depressed in the cathodic direction, as compared to the one without addition of LiCl, which demonstrates the inhibiting effect of the Cl^- anions.

The competitive effect of chloride anions on the deposition of cobalt in cobalt(II) thiocyanate is also shown by plotting the nucleation potential vs. the cathodic current measured at -2.2 V from cyclic voltammograms as a function of LiCl concentration (Fig. 8). The voltammetric measurements were carried out at scan rate of 20 mV/s in 0.1M $\text{Co}(\text{NCS})_2 + 0.5\text{M LiClO}_4$ DMF solution (the base solution) with several concentrations of LiCl. For the purpose of comparison, the same experiments were also performed in 0.1M $\text{CoCl}_2 + 0.5\text{M LiClO}_4$ DMF solution with addition of various concentrations of LiCl. The results are also shown in the figure. The nucleation potential and the cathodic current measured at a potential lower than the nucleation potential can reflect the difficulties of the nucleation and the rate of crystal growth for the deposition of cobalt in a DMF solution. In the base solution, it is worth noting that

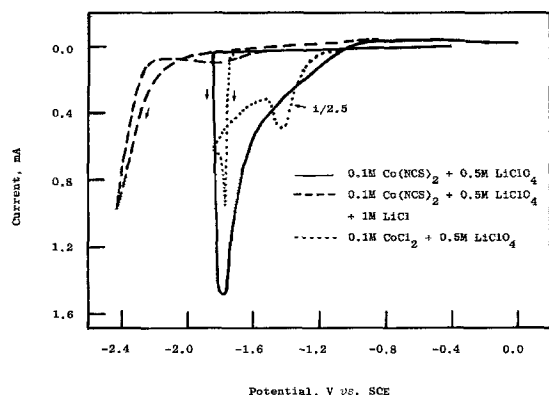


Fig. 7. Cyclic voltammograms for the deposition of cobalt from various cobalt(II) DMF solutions measured at a scan rate of 10 mV/s.

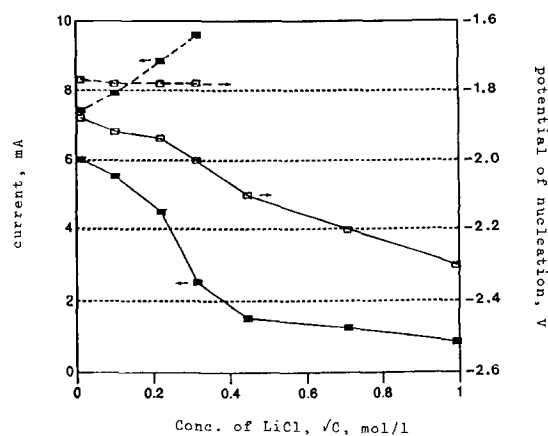


Fig. 8. Plots of the cathodic current measured at -2.2 V and the potential of nucleation against the square root of LiCl concentration added to 0.1M $\text{Co}(\text{NCS})_2 + 0.5\text{M LiClO}_4$ (—) and 0.1M $\text{CoCl}_2 + 0.5\text{M LiClO}_4$ (---). Scan rate = 20 mV/s.

the potential of nucleation shifts negatively and the cathodic current decreases as the concentration of Cl^- increases (solid curve in Fig. 8). This demonstrates the inhibiting effect of Cl^- anions on the deposition of cobalt from $\text{Co}(\text{NCS})_2$ DMF solution. However, such electrochemical behavior is quite different from the one observed in the CoCl_2 DMF solution. In 0.1M $\text{CoCl}_2 + 0.5\text{M LiClO}_4$ DMF solutions, the nucleation potential is independent of the Cl^- concentration and cathodic current increases as the concentration of chloride anions increases (dotted curves in Fig. 8). This again confirms that the deposition of cobalt in CoCl_2 occurs mainly through the electroreduction of $[\text{CoCl}_3(\text{DMF})_3]^-$ and the catalytic effect of Cl^- anions, which significantly enhances the rate of the deposition process via reduction of $[\text{CoCl}(\text{DMF})_5]^+$ (reactions [1]-[3]). The difference could be due to the fact that Cl^- anions added to $\text{Co}(\text{NCS})_2$ solution would reduce the concentration of $[\text{CoNCS}(\text{DMF})_5]^+$ through reaction [4]. Therefore, it seems more likely that the $[\text{CoNCS}(\text{DMF})_5]^+$ complex is the main electroactive species for the deposition of cobalt in $\text{Co}(\text{NCS})_2$ DMF solution



However, the reduction of the most stable species, $[\text{Co}(\text{NCS})_4]^{2-}$, takes place at more cathodic potential as compared to that for the electroactive species $[\text{CoNCS}(\text{DMF})_5]^+$. Therefore, the free NCS^- ions produced on the electrode surface have no catalytic effect on the deposition process, unlike Cl^- ions in CoCl_2 DMF systems (1).

The results shown so far indicate that the deposition of cobalt in nonaqueous solutions depends on the existence of cobalt(II) complexes with competitive ligands. In a $\text{Co}(\text{NCS})_2$ DMF solution, $[\text{CoNCS}(\text{DMF})_5]^+$ is the main electroactive species even though $[\text{Co}(\text{NCS})_4]^{2-}$ is the most stable complex component. The NCS^- anions released from the reduction of $[\text{CoNCS}(\text{DMF})_5]^+$ (reaction [6]) have no significant catalytic effect similar to that of the Cl^- anions for the deposition of cobalt in CoCl_2 DMF solution (1). The role of chloride anions in different cobalt solutions in DMF are summarized in Table I. The complex, $[\text{Co}(\text{DMF})_6]^{2+}$, exists in CoCl_2 solution, but not in $\text{Co}(\text{NCS})_2$ solutions, regardless of whether Cl^- is present or not. This demonstrates the greater coordination strength of thiocyanate ions compared to chloride ions. Although $[\text{Co}(\text{DMF})_6]^{2+}$ is not an electroactive species, the existence of the octahedral complex, $[\text{Co}(\text{DMF})_6]^{2+}$, could influence the catalytic function of the anions. Such a complex would be the source of the electroactive species through the substitute reaction of chloride ions (reaction [2]). Thus, the deposition behavior of cobalt in nonaqueous solutions depends not only on the electroactive complexes, but also on nonelectroactive complexes through the complexation equilibria.

The deposition mechanism of cobalt in $\text{Co}(\text{NCS})_2$ DMF solutions was also investigated using a pulse potential

Table I. Effect of Cl^- ions for the deposition in various cobalt(II) DMF solutions.

Solution Composition	$\text{Co}(\text{NCS})_2$ $[\text{CoNCS}(\text{DMF})_5]^+$ $[\text{Co}(\text{NCS})_4]^{2-}$	$\text{Co}(\text{NCS})_2 + \text{LiCl}$ $[\text{CoNCS}(\text{DMF})_5]^+$ $[\text{Co}(\text{NCS})_4]^{2-}$ $[\text{CoCl}_3(\text{DMF})]^-$ $[\text{CoNCS}(\text{DMF})_5]^+$ $[\text{CoCl}_3(\text{DMF})]^-$	CoCl_2 $[\text{Co}(\text{DMF})_6]^{2+}$ $[\text{CoCl}(\text{DMF})_5]^+$ $[\text{CoCl}_3(\text{DMF})]^-$ $[\text{CoCl}(\text{DMF})_5]^+$ $[\text{CoCl}_3(\text{DMF})]^-$
Electroactive species	$[\text{CoNCS}(\text{DMF})_5]^+$		
Effect of Cl^- ions Mechanism	Inhibition Electron transfer	Inhibition Electron transfer	Catalysis Catalysis

method. Figure 9 shows potentiostatic current-time transients measured at different pulse potentials in a $0.1\text{M Co}(\text{NCS})_2 + 0.5\text{M LiClO}_4$ DMF solution. It demonstrates that the cathodic current drops monotonically with time. Same current-time transient behavior has been observed in CoCl_2 aqueous solutions (14). This implies that the nucleation and crystal growth process for the deposition of cobalt in $\text{Co}(\text{NCS})_2$ DMF solutions are controlled by electron-transfer and mass-transfer reactions. This result is generally in agreement with the cyclic voltammetric behavior of the system. It also indicates that a steady-state condition could be achieved when the nickel disk electrode is almost or fully covered by cobalt crystallites. Thus, the interfacial area change caused by the nucleation and crystal growth process has little effect on the kinetics of the deposition process. This is indicated by the stable cathodic current when the potential becomes more cathodic. At this stage, the deposition process of cobalt in $\text{Co}(\text{NCS})_2$ DMF solution is under a mass-transfer process.

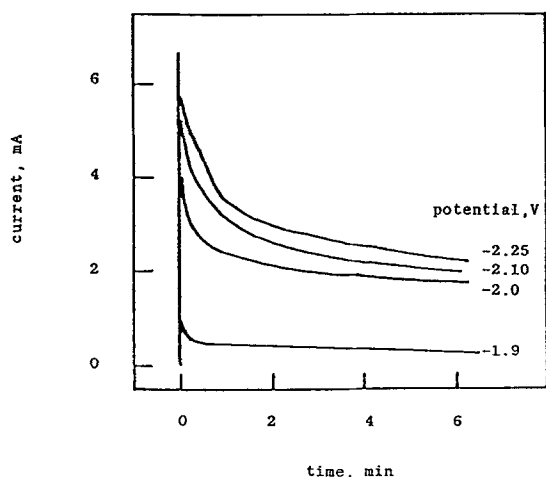


Fig. 9. Potentiostatic current-time transients from $0.1\text{M Co}(\text{NCS})_2 + 0.5\text{M LiClO}_4$ solution in DMF at various pulse potentials.

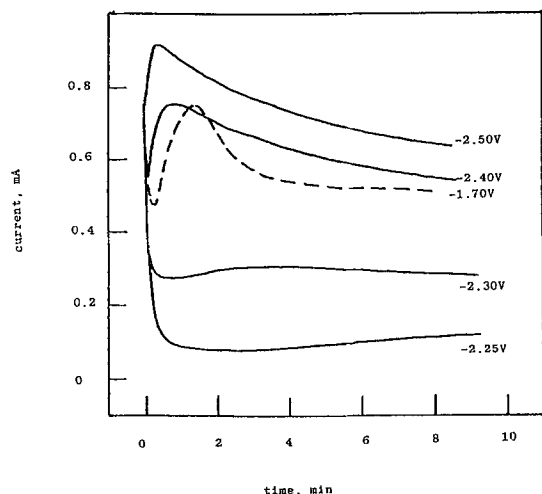


Fig. 10. Potentiostatic current-time transients from $0.1\text{M Co}(\text{NCS})_2 + 0.5\text{M LiClO}_4 + 1\text{M LiCl}$ solution in DMF at various pulse potentials. The dotted curve is performed from $0.1\text{M CoCl}_2 + 0.5\text{M LiClO}_4$ solution in DMF at pulse potential of -1.70 V .

Figure 10 illustrates the effects of Cl^- ions on the potentiostatic current-time transients measured in $0.1\text{M Co}(\text{NCS})_2 + 0.5\text{M LiClO}_4$ DMF solution (the base solution). With the addition of 1M LiCl to the base solution, the cathodic current shows a rise with time in the initial stages of the deposition. Similar behavior has been observed in $0.1\text{M CoCl}_2 + 0.5\text{M LiClO}_4$ DMF solution (dotted curve in Fig. 10). The transient current response measured in CoCl_2 DMF solutions is obviously due to the reduction of $[\text{CoCl}_3(\text{DMF})]^-$ complex (1). The indications are that a new electroactive species, $[\text{CoCl}_3(\text{DMF})]^-$, is formed as the result of adding Cl^- to $0.1\text{M Co}(\text{NCS})_2 + 0.5\text{M LiClO}_4$ solution in DMF. However, it was found that if the concentration of Cl^- ion is below 1M in the base solution, the current-time transients are the same as the ones observed in the base solution without addition of LiCl . The reason could be the very low concentration of the $[\text{CoCl}_3(\text{DMF})]^-$ formed. It seems that the formation of $[\text{CoCl}_3(\text{DMF})]^-$ due to the addition of chloride ions in $\text{Co}(\text{NCS})_2$ DMF solutions mainly depends on the relative Cl^-/NCS^- ion ratio. This again demonstrates that the deposition process of cobalt in DMF solution depends on the formation of electroactive species under the complexation equilibrium between the competitive ligands of anions.

Conclusions

In cobalt(II) thiocyanate DMF solutions, the cobalt(II) ions exist in the form of $[\text{CoNCS}(\text{DMF})_5]^+$ and $[\text{Co}(\text{NCS})_4]^{2-}$ with octahedral and tetrahedral structures, respectively. The most stable species is the $[\text{Co}(\text{NCS})_4]^{2-}$ complex. However, it has been found that for the electrodeposition of cobalt, the electroactive component is mainly $[\text{CoNCS}(\text{DMF})_5]^+$. It seems that the reduction of $[\text{Co}(\text{NCS})_4]^{2-}$ occurs at more cathodic potential in respect to that for the reduction of $[\text{CoNCS}(\text{DMF})_5]^+$. The mechanism for the deposition of cobalt in $\text{Co}(\text{NCS})_2$ DMF solutions is via under electron-transfer/mass-transfer control.

The addition of Cl^- ions to a $\text{Co}(\text{NCS})_2$ DMF solution decreases the concentration of $[\text{CoNCS}(\text{DMF})_5]^+$ and produces a chloro-complex with cobalt(II), $[\text{CoCl}_3(\text{DMF})]^-$. However, the effect of Cl^- ions as the competitive ligand is predominantly to decrease the concentration of the electroactive species, $[\text{CoNCS}(\text{DMF})_5]^+$. This leads to the inhibition of the nucleation and crystal growth process for the deposition of cobalt in the $\text{Co}(\text{NCS})_2$ DMF solution. This is in contrast with the deposition of cobalt from CoCl_2 DMF solutions. In that case, the increase in the concentration of the chloride ions at the electrode surface, either by addition of Cl^- or due to the electroreduction of cobalt chloro-complexes, will greatly increase the concentration of the electroactive species, therefore catalyzing the deposition process.

In general, the electrochemical behavior of metal electrodeposition in nonaqueous solution depends on the nature of metal ion complexes with the anions in the solution. That is, it depends not only on the forms of electroactive complexes, but also on the existence of other complex species under the complexation equilibrium between the competitive ligands of anions, which is very different from the deposition process of metal ions in aqueous solutions.

Acknowledgment

One of us (C.Q.C.) is in receipt of a British Council Split Ph.D. Research Scholarship and a Chinese Government Research Scholarship.

Manuscript submitted July 16, 1990; revised manuscript received Oct. 25, 1990.

REFERENCES

1. C. Q. Cui, S. P. Jiang, and A. C. C. Tseung, *This Journal*, **138**, 94 (1991).
2. V. Gutmann, "Coordination Chemistry in Non-Aqueous Solutions," Springer-Verlag, New York (1968).
3. S. Ishiguro, K. Ozutsumi, and H. Ohtaki, *J. Chem. Soc. Faraday Trans. I*, **84**, 2409 (1988).
4. W. Grzybowski and M. Pilarczyk, *ibid.*, **82**, 1703 (1986).
5. W. Grzybowski and M. Pilarczyk, *ibid.*, **82**, 1745 (1986).
6. M. Pilarczyk, W. Grzybowski, and L. Klinszporn, *ibid.*, **83**, 2261 (1987).
7. W. E. Waghorne and H. Rubalcava, *ibid.*, **78**, 1199 (1982).
8. J. E. Coetzee, *Pure Appl. Chem.*, **49**, 877 (1977).
9. L. Sestilli, C. Furlani, and G. Festucia, *Inorg. Chim. Acta*, **4**, 542 (1970).
10. C. Q. Cui, S. P. Jiang, and A. C. C. Tseung, *This Journal*, **137**, 3418 (1990).
11. I. Bimaghra and J. Crousier, *Mater. Chem. Phys.*, **21**, 109 (1989).
12. S. Fletcher, C. S. Halliday, D. Gates, M. Westcott, T. Lwin, and G. Nelson, *J. Electroanal. Chem.*, **159**, 267 (1983).
13. A. J. Bard and L. R. Faulkner, "Electrochemical Methods: Fundamentals and Applications," John Wiley & Sons, New York (1980).
14. C. Q. Cui, Essex University, Internal Report "Electrodeposition of Co in Chloride Aqueous Solutions," May, 1989.

Preparation and Characterization of Amorphous and Crystalline Electrodeposited Chromium-Nickel-Carbon Alloys

Rung-Ywan Tsai

Materials Research Laboratories, Industrial Technology Research Institute, Hsinchu, Taiwan, China

Shinn-Tyan Wu

Department of Materials Science and Engineering, National Tsing Hua University, Hsinchu, Taiwan, China

ABSTRACT

Amorphous and crystalline chromium films with varying amounts of nickel and carbon are electrodeposited from the chromic acid electrolyte containing formic acid. Auger electron spectroscopy analysis shows an almost homogeneous distribution of the alloying elements through the film thickness. When the carbon content within the film is higher than 3.29 w/o the film is amorphous; otherwise, it is crystalline. The hardness of the deposits decreases with increasing Ni content. The hardening of the amorphous film by annealing at 500°C for 1 h is shown to be related to the uniform distribution of submicron α -Cr and $(\text{Cr,Ni})_{23}\text{C}_6$ grains within the amorphous matrix.

Electrodeposited alloys of chromium and Fe, Ni, and Co exhibit good corrosion resistance, high strength and hardness, and also retain strength at high temperature (1). There has been a great deal of research on the development of a suitable process to electrodeposit these alloys. Cr-Ni alloys were usually deposited from the electrolytes containing trivalent chromium and various complexing agents (2-4). Hexavalent chromium electrolytes used for Cr-Ni alloys do not seem to yield thick coatings (5).

A characteristic of electrodeposited films, which differs from those films produced by other means, is the extent to which extremely small amounts of chemical agents (often organic) can significantly influence the structure and properties. It has been known that electrodeposited chromium could be hydrides (β -Cr and τ -Cr) (6, 7) or amorphous phase (8-10) if formic acid or other certain organics were added to the sulfate-catalyzed chromic acid electrolyte or the trivalent chromium sulfate solution (11). From the results of measurement of the compositions of the deposits including carbon, hydrogen, oxygen, and nitrogen, we proposed that the carbon interstitials in the deposits, originating from the formic acid, play the key role in determining the relative stability of α , β , and amorphous Cr (12). The hardness of the amorphous Cr film can be increased from 1000 Hv to above 1600 by annealing at 500°C for 1 h (10, 11). This is in contrast to the conventional hard chromium plating which softens on heating. With the aid of x-ray diffraction (XRD), differential thermal analysis (DTA), and transmission electron microscopy (TEM), it has been found that the increase of hardness during the heat-treatment was due to the crystallization of chromium and its carbides (13).

It has been reported (14) that the glass formation ability of Cr-C alloys prepared by the liquid-quenched method can be increased by adding certain alloy elements, such as Ni, Fe, or Co. However, the hardness and crystallization temperature of these amorphous alloys decrease with increasing Ni, Fe, and Co contents. Similar results have been found by us in electrodeposited Cr-Fe-C ternary alloy films (15).

In this paper we report the preparation of amorphous and crystalline Cr films with varying amounts of nickel and carbon from the hexavalent chromium electrolytes containing formic acid. The thermal stability of these films was analyzed by DTA. The morphology was studied by SEM. The microstructure of the as-deposited and annealed films were characterized by means of XRD and TEM analysis. The effect of microstructure on the hardness of the annealed amorphous Cr-Ni-C films is also discussed.

Experimental Procedure

The films of Cr-Ni-C alloys were electrodeposited from an electrolyte containing 100 g/liter of chromic acid, 100 g/liter of nickel sulfate hexahydrate, 40 g/liter ammonium sulfate, and 30 ml/liter of an 85% solution of formic acid at a current density of 50 A/dm² for 90 min. All the chemicals were reagent grade. The water was deionized. The bath temperatures were controlled at a range of 30-60°C. The plating cell was a 500 ml beaker containing 300 ml of electrolyte. The anodes were two facing lead-5% antimony alloy plates of the dimensions 80 × 50 × 6 mm³. They were situated vertically at the ends of the plating cell. The substrates were low carbon steel strips of the dimensions 40 × 10 × 0.2 mm³ which were located at the center of the cell.